Six-degree-of-freedom three-Wheeled-vehicle model validation

T.R. Gawade
Research Scholar, Department of Mechanical Engineering, IIT Delhi, India.
S. Mukherjee*
Associate Professor, Department of Mechanical Engineering, IIT Delhi, India.
D. Mohan
Professor, TRIPP, IIT Delhi, India.

Abstract:

A spatial six-degree of freedom (DOF) mathematical model of a Three-Wheeled Vehicle (TWV) used extensively in Asian countries is developed. The governing equations are derived and integrated explicitly without liberalization to yield a large deformation model that can be used for parametric studies. The model includes suspension model, tire compliance, lateral force due to cornering stiffness and rolling resistance at the tire. The model is validated against vertical accelerations measured when passing over a road bump. The lateral motion is validated through a steady state circular test procedure.

Keywords: Three-Wheeled Vehicle, magic formula, Euler angles, road bump, steady state circular test, wheel lift-off, model validation

1 INTRODUCTION

Three-Wheeled Vehicles (referred as TWV in this paper) form an essential part of public transport for the urban middle class population of India. Apart from India, TWVs are also being used world over for public transport and for carrying freight. Based on statistical data, the poor stability of the three-wheeled ATVs, which are used for recreation and fun, is frequently cited as an important factor in accidents **[1]**. Relatively higher centre of gravity, the lack of differential for the driving rear axle have been cited as contributors to rollovers. Very few publications evaluate the performance of TWVs in everyday use for mass transportation.

An extensive review of the contribution of vehicle dynamics theory to practical vehicle design is available **[2]**. The role of actively controlled components, for example active suspension, four-wheel steering, and their impact on vehicle performance and safety has been discussed. A six DOF mathematical model of a three-wheeled ATV/rigid rider system without suspension has been developed. Even though rigid body simulators like Madymo™ are available to carry out simulations, parametric variation study can be done more effectively using such customised codes. Simulation of ATV passing over three bump profiles, of rectangular, parabolic and sinusoidal shapes has been presented **[3,4]**. A longer ramp-like bump profile disturbed the vehicle/rider system more than a shorter length bump profile of the same height. The three different profiles evaluated had varying span with same height at the middle of the span.

The kind of TWV considered in this paper has been evaluated for ride characteristics and a better design is proposed based on the sensitivity analysis of suspension stiffness and damping **[5,6,7]**. No verification of the model or the derivation of the model has been presented, and the work concentrates on the ride characteristics over a road profile characterized by auto-power spectral density.

* *Correspondence author: Associate Professor, Department of Mechanical Engineering, IIT Delhi, India. E-mail sudipto@mech.iitd.ernet.in, Ph. No. 91-11-26591138*

In this paper, the mathematical model of a three-wheeled vehicle with suspension and compliant tires is presented. In variance to liberalized models available in literature, the mathematical methodology presented here integrates the Euler Equations **[8]** explicitly and hence valid for large displacement analysis. Large vertical displacement input in the form of road bumps was used to verify the model. The instrumented TWV was run over road bumps and measured vertical acceleration compared with the results of TWV mathematical model for validation.

The parameters for physical model of TWV, and the theoretical approach adopted for model building is detailed. The acceleration of TWV running over the bump, without steering, the simulation results are plotted in time domain. However, the equations of motion can take into account the steering effect if required for further analysis as it is done in the steady state circular test section.

In the experimental set-up section the instrumentation used for digital capturing of vertical acceleration signal is described. Fast Fourier Transform (FFT) using MATLAB® code and data filtering using Butterworth filter available in LabVIEW™ Virtual Instrument (VI) are discussed. The actual data along with filtered data has been overlapped for comparison.

Discrepancies in the results obtained from theoretical model and experimental results are reported in the comparison section. Based on match between results of theoretical model and experimentation, it is proposed that the present mathematical model of TWV can be used to evaluate further aspects of stability analysis.

2 THEORETICAL TWV MODEL

Bajaj Auto rickshaw-Rear Engine 4 Stroke, Petrol model manufactured by Bajaj Auto Limited, shown in Fig. 1, is mathematically modeled. The corresponding spatial discrete element model along with the forces acting is shown in Fig. 2. The body of the vehicle has been modelled with six DOF– three linear motion along x, y and z-axes and three rotational motions about three axes (roll-pitch-yaw). Collective mass of three wheels is 6.5 percent of the total mass of vehicle system including two occupants- a driver and a passenger and hence has been neglected. This is comparatively very less, so to simplify the model, wheels have not been modelled separately. As shown in Fig. 3 the front suspension consists of spring, damper and wheel mounted on a stiff member pivoting about the front fork and not coaxially. The effective coaxial suspension parameters (k_{f1} and c_{f1} in Fig. 2) to account for the suspension mechanism have hence been computed from the manufacturer's data.

Vehicle attitude and trajectory through the course of maneuver are defined with respect to a right hand orthogonal axis system, inertial frame (QXYZ) that is fixed to the earth. Origin of moving reference Gxyz coincides with center of mass of vehicle body and travels with the vehicle. The frame is well known as body-centered frame. The co-ordinates showed in Fig. 2 are displacements along x, y, z-axes. Angular velocities of body centered frame ω_x, ω_y and ω_z are about x, y, z-axes respectively. The vehicle motion is described by the three linear displacements along inertial X, Y and Z-axes and three angular displacements which are the Euler angles ψ, β and θ.

Fig. 1 Bajaj Auto rickshaw- rear engine 4 stroke, petrol model

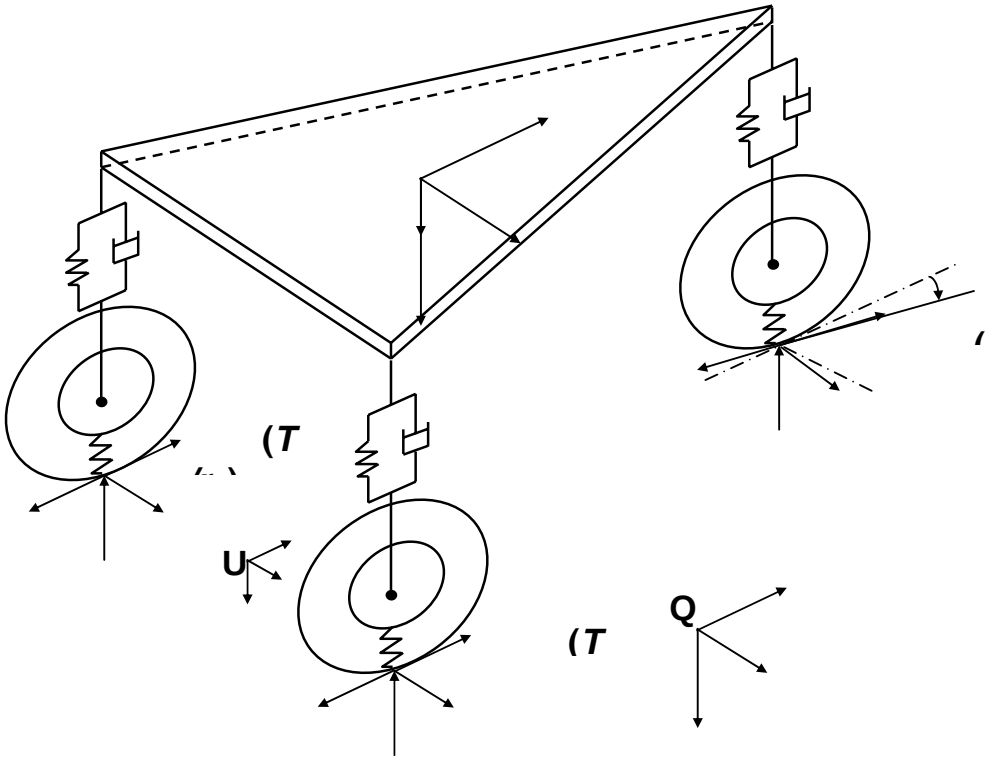

Fig. 2 Discrete element model of TWV

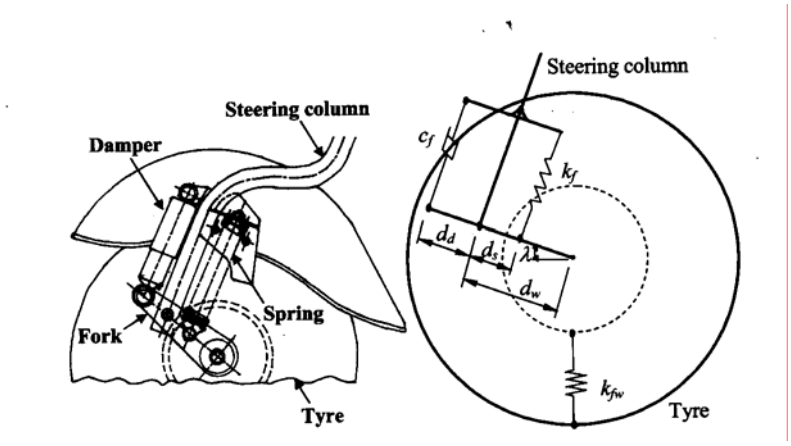

Fig. 3 Front wheel suspension (d_d=0.052 m, d_s=0.034 m, d_w=0.086 m, λ=38 deg)

Three independent Euler angles are used to describe the orientation of body centered frame Gxyz in relation to an inertial frame. The transformation matrix is developed based on these rotations. Euler angles involve three successive rotations about three axes that are not orthogonal in general. The concept of yaw, pitch and roll angles is used while selecting axes for rotations. Initially the inertial frame is selected to coincide with body-centered frame. Beginning at the inertial frame, the axis system is first rotated in yaw (angle ψ around the current z-axis which is aligned with Z-axis), then in pitch (angle β around the new y-axis) and then in roll (angle θ around the new x-axis) to line up with the body-centered frame. The triple (ψ, β, θ) is said to be representation of yaw, pitch and roll angles

of orientation of body-centered frame Gxyz, with respect to inertial frame QXYZ. It is necessary to adhere strictly to the defined sequence of rotations, because finite rotations of vectors do not generally obey the commutative law of vector addition. A vector $\{V\}$ expressed in these co-ordinate systems would have components expressed by matrix transformation $[T]$, as follows:

$$\{V_{XYZ}\} = [T]\{V_{xyz}\} \tag{1}$$

Where $[T] = [R_\psi][R_\beta][R_\theta]$ and $[R]$ is a rotation matrix.

The angular velocities (ω_x, ω_y and ω_z) about the body attached axes after three rotation in a sequence are,

$$\omega_x = \dot{\theta} - \dot{\psi}\sin\beta \tag{2}$$

$$\omega_y = \dot{\beta}\cos\theta + \dot{\psi}\cos\beta\sin\theta \tag{3}$$

$$\omega_z = -\dot{\beta}\sin\theta + \dot{\psi}\cos\beta\cos\theta \tag{4}$$

Simple differentiation of angular velocity components (scalar quantities) with respect to time leads to angular acceleration components $\dot{\omega}_x, \dot{\omega}_y$ and $\dot{\omega}_z$. Therefore, the angular accelerations about the body attached axes are as follows:

$$\dot{\omega}_x = \ddot{\theta} - \ddot{\psi}\sin\beta - \dot{\psi}\dot{\beta}\cos\beta \tag{5}$$

$$\dot{\omega}_y = \ddot{\beta}\cos\theta - \dot{\beta}\dot{\theta}\sin\theta + \ddot{\psi}\cos\beta\sin\theta - \dot{\psi}\dot{\beta}\sin\beta\sin\theta + \dot{\psi}\dot{\theta}\cos\beta\cos\theta \tag{6}$$

$$\dot{\omega}_z = \ddot{\psi}\cos\beta\cos\theta - \dot{\psi}\dot{\beta}\sin\beta\cos\theta - \dot{\psi}\dot{\theta}\cos\beta\sin\theta - \ddot{\beta}\sin\theta - \dot{\beta}\dot{\theta}\cos\theta \tag{7}$$

2.1 Force Balance Equations for TWV

The force balance or Newton's equation for a rigid mass system is the generalization of Newton's second law for the motion of a particle.

$$F = m\bar{a} \tag{8}$$

Where F is the force on the rigid mass system represented in an inertial frame, $\bar{a}$ is the acceleration of the center of mass of the rigid body in inertial frame and m is total mass of rigid body which is time invariant. This equation states that the resultant of the external forces (F_x, F_y and F_z) on any system of mass equals the total mass of the system times the absolute acceleration of the center of mass.

$$\begin{bmatrix} F_x \\ F_y \\ F_z \end{bmatrix} = m\begin{bmatrix} \bar{a}_x \\ \bar{a}_y \\ \bar{a}_z \end{bmatrix} = m\begin{bmatrix} \ddot{X} + \omega_y\dot{Z} - \omega_z\dot{Y} \\ \ddot{Y} + \omega_z\dot{X} - \omega_x\dot{Z} \\ \ddot{Z} + \omega_x\dot{Y} - \omega_y\dot{X} \end{bmatrix} \tag{9}$$

Finally, the equations of motion for the vehicle system are given as follows,

$$\ddot{X} = \frac{F_x}{m} + \omega_z\dot{Y} - \omega_y\dot{Z} \tag{10}$$

$$\ddot{Y} = \frac{F_y}{m} + \omega_x\dot{Z} - \omega_z\dot{X} \tag{11}$$

$$\ddot{Z} = \frac{F_z}{m} + \omega_y \dot{X} - \omega_x \dot{Y} \tag{12}$$

Forces in local frame/body attached frame ($F_x^{'}, F_y^{'}$ and $F_z^{'}$) are transferred to inertial frame by transformation $[T]$ as follows:

$$\begin{bmatrix} F_x \\ F_y \\ F_z \end{bmatrix} = [T] \begin{bmatrix} F_x' \\ F_y' \\ F_z' \end{bmatrix} \tag{13}$$

The external forces acting on body, represented in a body attached frame are given by,

$$F_x' = \left(\frac{T_f}{r_w} - F_f \right) \cos\delta - \left(F_{rr} + F_{rl} \right) + \frac{T_{rr} + T_{rl}}{r_w} - L_f \sin\delta \tag{14}$$

$$F_y' = \left(\frac{T_f}{r_w} - F_f \right) \sin\delta + L_f \cos\delta + L_{rr} + L_{rl} \tag{15}$$

$$F_z' = mg - \left(N_f + N_{rr} + N_{rl} \right) \tag{16}$$

Where

F = the rolling friction at the wheel,

T = the torque applied at the wheel,

δ = the steering angle,

L = the lateral force at the wheel,

N = the normal reaction exerted by the road on the wheel,

g = the gravitational constant,

Subscripts *f*, *rr* and *rl* are used for front wheel, rear right wheel and rear left wheel respectively.

Frictional forces at the three wheels (front, right and left) are proportional to the normal reactions **[9]**. The constant of proportionally is called as the coefficient of rolling friction (μ_r), which is taken as 0.017 here. The frictional forces due to rolling are given by,

$$F_f = \mu_r N_f \tag{17}$$

$$F_{rr} = \mu_r N_{rr} \tag{18}$$

$$F_{rl} = \mu_r N_{rl} \tag{19}$$

Reactions exerted by ground on the three wheels (front, right and left) are given by,

$$N_f = \frac{mgb}{l} + k_{fe} z_f' + c_{f1} \dot{z}_f' \tag{20}$$

$$N_{rr} = \frac{mga}{2l} + k_{rre} z_{rr}' + c_{rr} \dot{z}_{rr}' \tag{21}$$

$$N_{rl} = \frac{mga}{2l} + k_{rle} z_{rl}' + c_{rl} \dot{z}_{rl}' \tag{22}$$

where k_{fe} and c_{f1} are the equivalent spring stiffness and equivalent damping coefficient, respectively, for front wheel suspension system (Fig. 3). Similarly k_{rre} and k_{rle} are the equivalent spring stiffness for the rear right wheel and the rear left wheel, respectively.

Vertical displacement to individual wheel has an input through a text file that contains the data of horizontal distance and the corresponding vertical rise/fall over the bump profile. This was obtained from measurements of the bumps present on local roads and shown in Fig. 4. The deflections of the suspensions (z'_f, z'_{rr} and z'_{rl}) are given as follows and the allowable maximum deflection values are given in Table 1.

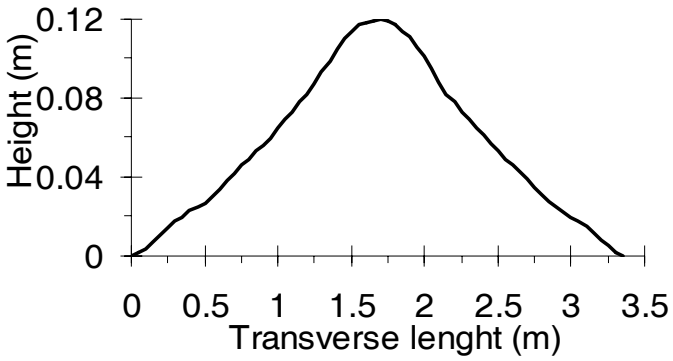

Fig. 4 Bump profile

$$z'_f = z - a\sin\beta - z_f \tag{23}$$

$$z'_{rr} = z + b\sin\beta + c\sin\theta - z_{rr} \tag{24}$$

$$z'_{rl} = z + b\sin\beta - c\sin\theta - z_{rl} \tag{25}$$

The relative velocities experienced by the suspensions of the vehicle body ($\dot{z}'_f$, $\dot{z}'_{rr}$ and $\dot{z}'_{rl}$) are given as follows:

$$\dot{z}'_f = \dot{z} - a\dot{\beta}\cos\beta - \dot{z}_f \tag{26}$$

$$\dot{z}'_{rr} = \dot{z} + b\dot{\beta}\cos\beta + c\dot{\theta}\cos\theta - \dot{z}_{rr} \tag{27}$$

$$\dot{z}'_{rl} = \dot{z} + b\dot{\beta}\cos\beta - c\dot{\theta}\cos\theta - \dot{z}_{rl} \tag{28}$$

The lateral force of TWV tires for different slip angles has been calculated based on the 'magic formula' [**10**] in the simulation to allow the tyre behaviour to be modelled over the whole range of slip angles and vertical loads. The parameters are set to match a limited quantity of experimental data available for small tires [**11**]. The basic form of this magic formula [**10**] is given by,

$$L(\alpha) = D\sin\{C\arctan[B\alpha - E(B\alpha - \arctan(B\alpha))]\} \tag{29}$$

Figure 5 shows the variation of the lateral force exerted by the tire against the slip angle. The lateral force applied by the road on the tire is assumed positive in the direction of the y axis, and the slip angle measured about the z axis. The stiffness factor B, the shape factor, the peak factor D, the curvature factor E and the slip angle α can be deduced from the variation shown in figure 5.

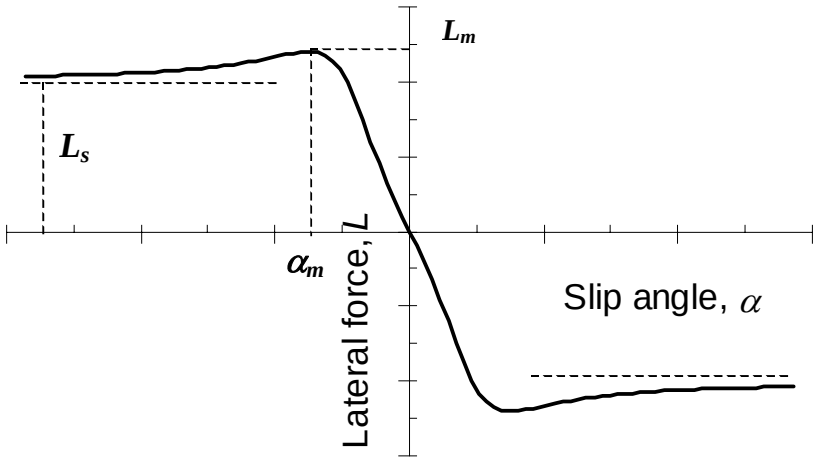

Fig. 5 Lateral Force on tire vs slip angle

$$B = (CD)^{-1}\left(dL/d\alpha\right)_{\alpha=0} \tag{30}$$

$$C = 2 - (2/\pi)\arcsin\left(L_s/L_m\right) \qquad (>0) \tag{31}$$

$$D = L_m \tag{32}$$

$$E = \frac{B\alpha_m - \tan\left(\pi/2C\right)}{B\alpha_m - \arctan\left(B\alpha_m\right)} \tag{33}$$

The slope of curve at α equal to zero, $\left(dL/d\alpha\right)$, is conventionally called the cornering stiffness. The average peak lateral force, $\left(L_m\right)$, is taken to be 0.8 times the normal reaction and the sliding lateral force, $\left(L_s\right)$, 0.75 times the normal reaction for the testing conditions. If the slip angles are small then they can be written as a ratio of local lateral velocity to the local linear velocity as **[12],**

$$\alpha_f = \left(\frac{\dot{y} + a\omega_z}{\dot{x}} - \delta\right) \tag{34}$$

$$\alpha_{rr} = \left(\frac{\dot{y} - b\omega_z}{\dot{x} - c\omega_z}\right) \tag{35}$$

$$\alpha_{rl} = \left(\frac{\dot{y} - b\omega_z}{\dot{x} + c\omega_z}\right) \tag{36}$$

The lateral forces are the restoring forces in case of maneuvering the vehicle. So the lateral forces acting on each wheel are given by,

$$L_f = -L(\alpha)_{\alpha=\alpha_f} \tag{37}$$

$$L_{rr} = -L(\alpha)_{\alpha=\alpha_{rr}} \tag{38}$$

$$L_{rl} = -L(\alpha)_{\alpha=\alpha_{rl}} \tag{39}$$

2.2 Euler's equations of Rotation for TWV

Initially, the triangular frame of TWV is horizontal and parallel to the ground. It yaws about z-axis, pitches about new y-axis and rolls about new x-axis, finally giving ω_x and ω_y and ω_z as yaw, pitch and roll angular velocities respectively. The TWV body is shown (Fig. 2) at instantaneous time (t) that is obtained by three successive rotations defined by Euler's angles. The angular components ω_x, ω_y and ω_z are general functions of time because orientation of frame Gxyz is time variant. Therefore, the angular velocities permit simple differentiations with respect to time, to get instantaneous rates of change of angular velocities $\dot{\omega}_x, \dot{\omega}_y$ and $\dot{\omega}_z$ respectively. These components of angular acceleration of the body-centered axes are required for the moment/Euler's equations. The moments (M_x, M_y and M_z), moment of inertia (I_{xx}, I_{yy} and I_{zz}) and products of inertia (I_{xy}, I_{yz} and I_{xz}) are time invariant as x-y-z is fixed to body. Therefore the moments are given as follows:

$$M_x = \dot{\omega}_x I_{xx} + \omega_y \omega_z \left(I_{zz} - I_{yy}\right) + I_{xy}\left(\omega_z \omega_x - \dot{\omega}_y\right) - I_{xz}\left(\dot{\omega}_z + \omega_y \omega_x\right) - I_{yz}\left(\omega_y{}^2 - \omega_z{}^2\right) \quad (40)$$

$$M_y = \dot{\omega}_y I_{yy} + \omega_z \omega_x \left(I_{xx} - I_{zz}\right) + I_{yz}\left(\omega_x \omega_y - \dot{\omega}_z\right) - I_{yx}\left(\dot{\omega}_x + \omega_z \omega_y\right) - I_{zx}\left(\omega_z{}^2 - \omega_x{}^2\right) \quad (41)$$

$$M_z = \dot{\omega}_z I_{zz} + \omega_x \omega_y \left(I_{yy} - I_{xx}\right) + I_{zx}\left(\omega_y \omega_z - \dot{\omega}_x\right) - I_{zy}\left(\dot{\omega}_y + \omega_x \omega_z\right) - I_{xy}\left(\omega_x{}^2 - \omega_y{}^2\right) \quad (42)$$

Cross products of inertia terms (I_{xy} and I_{yz}) will be absent when the vehicle body is symmetrical about a longitudinal-vertical plane (Gxz). And the moments are reduced to following form.

$$M_x = \dot{\omega}_x I_{xx} + \omega_y \omega_z \left(I_{zz} - I_{yy}\right) - I_{xz}\left(\dot{\omega}_z + \omega_y \omega_x\right) \quad (43)$$

$$M_y = \dot{\omega}_y I_{yy} + \omega_z \omega_x \left(I_{xx} - I_{zz}\right) - I_{zx}\left(\omega_z^2 - \omega_x^2\right) \quad (44)$$

$$M_z = \dot{\omega}_z I_{zz} + \omega_x \omega_y \left(I_{yy} - I_{xx}\right) + I_{zx}\left(\omega_y \omega_z - \dot{\omega}_x\right) \quad (45)$$

The external moments acting on body, represented in a body attached frame are given by,

$$M_x = \left(\left(F_f - \frac{T_f}{r_w}\right)\sin\delta - L_f \cos\delta\right)\left(h - z'_f\right) - L_{rr}\left(h - z'_{rr}\right) - L_{rl}\left(h - z'_{rl}\right) + \left(N_{rl} - N_{rr}\right)c \quad (46)$$

$$\begin{aligned} M_y = {} & \left(\frac{T_f}{r_w} - F_f\right)\cos\delta\left(h - z'_f\right) + \left(\frac{T_{rr}}{r_w} - F_{rr}\right)\left(h - z'_{rr}\right) - L_f \sin\delta\left(h - z'_f\right) \\ & + \left(\frac{T_{rl}}{r_w} - F_{rl}\right)\left(h - z'_{rl}\right) + N_f a - \left(N_{rr} + N_{rl}\right)b \end{aligned} \quad (47)$$

$$M_z = \left(\left(\frac{T_{rl} - T_{rr}}{r_w}\right) + F_{rr} - F_{rl}\right)c + \left(L_f \cos\delta + \left(\frac{T_f}{r_w} - F_f\right)\sin\delta\right)a - \left(L_{rr} + L_{rl}\right)b \quad (48)$$

Equations of motion (13) and (43) to (45) are simulated using an implementation of explicit Runge-Kutta (4,5) pair, in MATLAB® as “ode45”. The simulation results are presented next.

3 SIMULATION OVER BUMP

The TWV model was passed over the bump having 3.35 m transverse length and 0.12 m peak height at longitudinal velocity equal to 8.5 m/s. Following results were obtained using

parameters listed in Table 1 and suspension data, i.e. spring and damper properties shown in Fig. 6 to Fig. 9. Appendix A shows the calculations for center of gravity (CG) and mass moment of inertia. Some of the data was available from the manufacturer; remaining was obtained after necessary tests and measurements. Fig. 10 shows simulation result of vertical acceleration in time domain, in the driver's compartment beneath the seat, on Y-member of frame. In Fig. 11, the plot of suspensions' deflection (z'_f, z'_{rr} and z'_{rl}) at each corner of TWV body and the bottoming and full extension of individual suspensions are clearly visible. The plot of pitch angle variation is shown in Fig. 12 that reflects the TWV nose-up and down behavior. The plot of reactions (N_f, N_{rr} and N_{rl}) exerted by ground on individual wheels of TWV is shown in Fig. 13. The wheel lift-off over bump occurs when the reaction exerted on the wheel(s) becomes zero. If the wheel(s) lifts-off, the present set of equations of motion are modified with the reaction set to zero. Additionally there is no resistance to motion along the longitudinal direction and lateral direction, at the wheel(s), which lose contact with the ground. The sequence of events as the TWV passes over the bump is:

Section A-B: Front wheel impacts the bump during ascent, imparting vertical acceleration to the chassis. Front suspension compresses and eventually bottoms-out, pitching the nose upward.

Section B-C: Front wheel starts its descent over the bump; pitches nose down. The normal reaction exerted by the ground reduces and the wheel leaves the bump when the reaction goes to zero.

Section D-E: Rear wheels impact the bump during ascent, the chassis continues with the nose pitching downward.

Section E-F: Rear wheels descend over the bump; and eventually loose contact with the ground. Rear suspensions are fully extended for most of the later part of this duration.

During section D-C front wheel descends and rear wheel ascends, pitching the nose down. At F all the wheels have traversed the bump, and there is a large impact on the plane road after the bump. Front suspension bottoms-out, the rear suspension is compressed but does not bottom-out. The nose of the TWV pitches upward. At G the fluctuations in vertical acceleration are observed to die out.

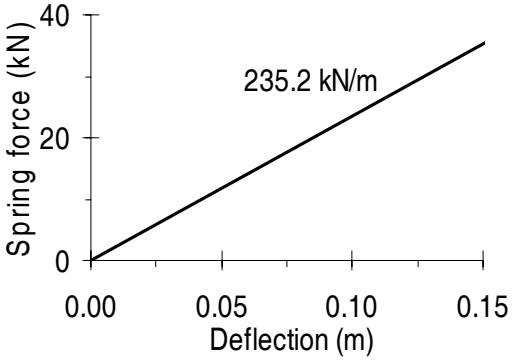

Fig. 6 Front spring characteristics (k_f)

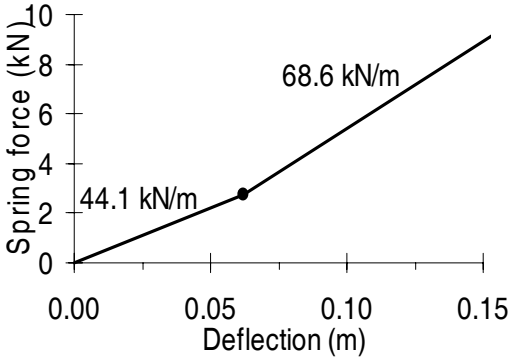

Fig. 7 Rear spring characteristics (k_{rr} or k_{rl})

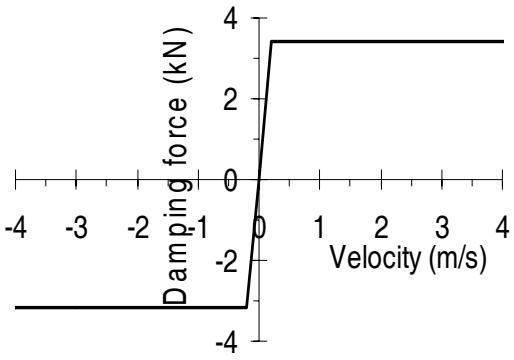

Fig. 8 Front damper characteristics (c_f)

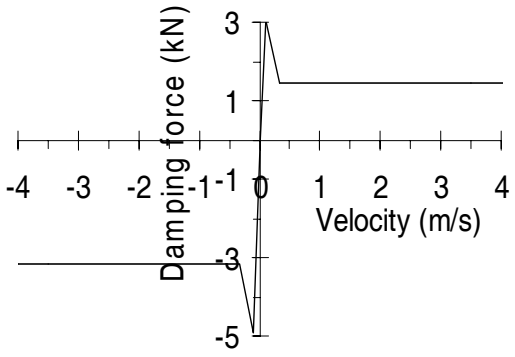

Fig. 9 Rear damper characteristics (c_{rr} or c_{rl})

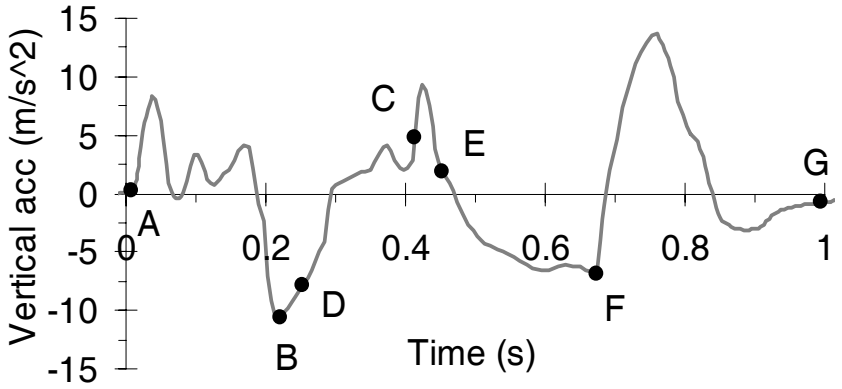

Fig. 10 Simulation result- Vertical acceleration in time domain

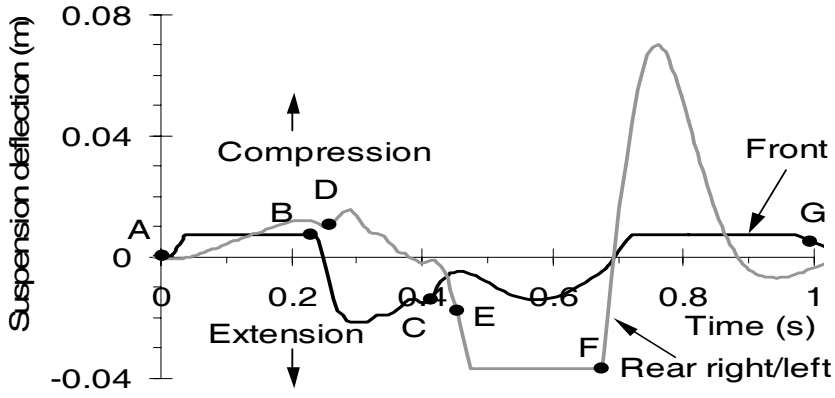

Fig. 11 Suspension deflection

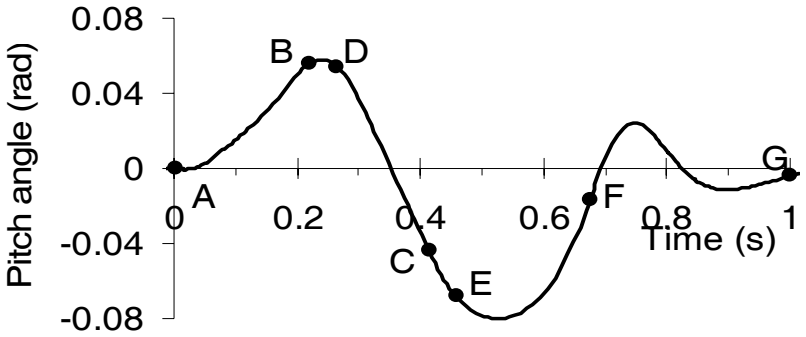

Fig. 12 Pitch angle variation

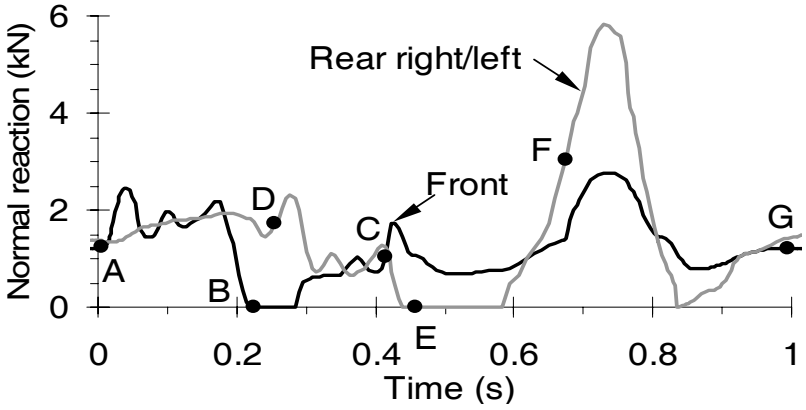

Fig. 13 Normal reactions at each wheel

4 STEADY STATE CIRCULAR TEST

As reported in **[13]**, the ISO 4138 procedure requires the test vehicle to be driven on a path of known radius. The analysis of this maneuver had the aim of identifying the steer angle associated with the assumed steady turn. The vehicle was simulated at an initial forward speed of 10 m/s and allowed to travel along the curve without any torque input at the wheels. A steering angle of 0.15 rad (approximately equal to 8.6 deg) was used in this simulation. The circular path negotiated by the TWV is shown in Fig. 14. The average radius of the circular path traced was found to be 13.62 m. Geometry in Fig. 15 shows that the steer angle (δ) may be represented by the following equation,

$$\sin \delta = l / r \tag{49}$$

where r and l represent the radius of turn and wheel base, respectively. Using equation (49) turn radius comes out to be 13.38 m. The radius of circle traced in simulation is greater than the theoretically predicted radius by an amount of 0.24 m (1.8%). The radius of the circular path traced being greater indicates a tendency of understeer, and the conformity to the theoretical value verifies the lateral behavior of the simulation.

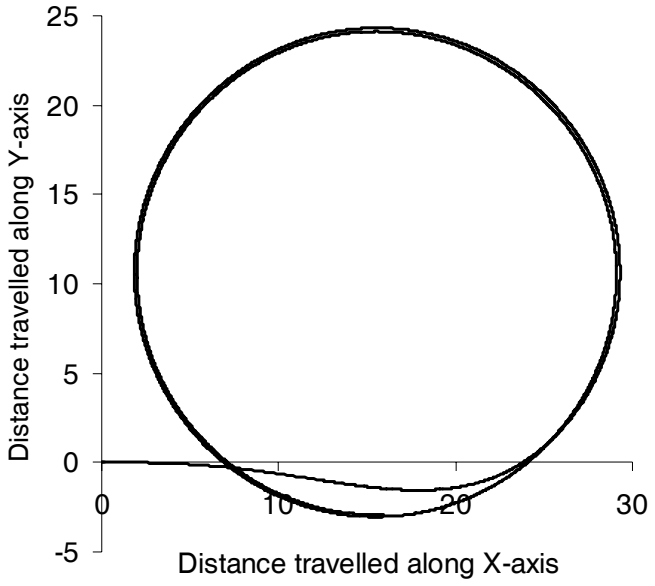

Fig. 14 Steady state circular test

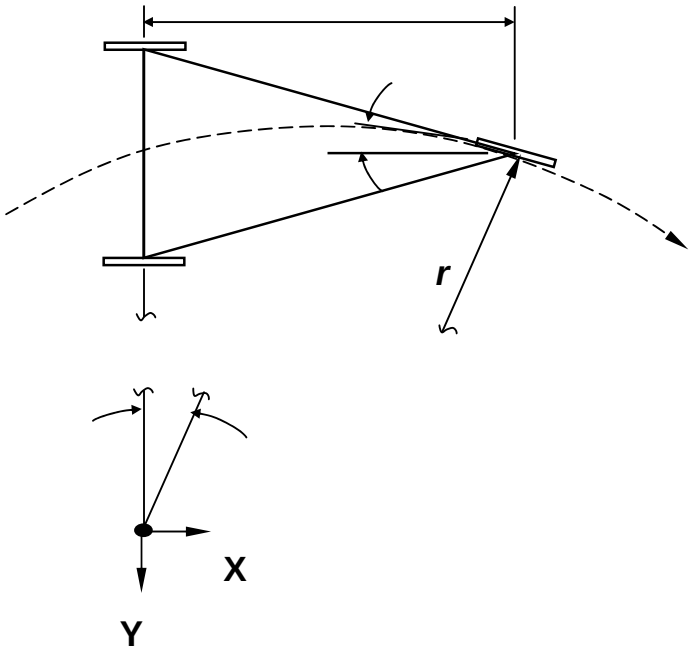

Fig. 15 Geometry of TWV for steady state circular test

5 EXPERIMENTAL SET-UP: FOR MEASUREMENT OF VERTICAL ACCELERATION

In the present study, vertical acceleration measurement of TWV while passing over bump was performed with B&K Delta Shear Piezoelectric accelerometer (type 4371) and charge amplifier (type 2635). The acceleration was sampled at 200 Hz with a PICO data acquisition card (ADC212). Observed frequencies were up to 16 Hz, eliminating requirements of higher sampling rates. The experimental set-up of instrumentation is shown in Fig. 16. The complete instrumentation was fixed in a box with a hard base having flexible clamps and then positioned on TWV's passenger seat. The recordings were done on TWV (Bajaj Auto Rickshaw rear petrol engine, three wheeler) driven on road with bumps of varying transverse length and height, at varying speeds.

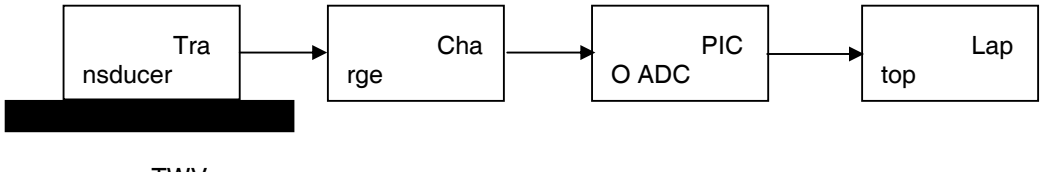

Fig. 16 Experimental set-up for vertical acceleration measurement

The bump profile analyzed here has a transverse length of 3.35 m and height 0.12 m (Fig. 4). The vehicle speed was determined to be 8.5 m/s using stopwatch measurements. For the test, the driver and a rear seat occupant were present for a total weight of 403.87 kg. Vertical acceleration in the driver's compartment beneath the seat, on Y-member of frame was monitored and the data captured when the TWV passed over the bump.

The acquired data is presented in Fig. 17 as signal before filtering. Frequency spectrum of vertical acceleration was obtained using the "fft" function in Matlab and is shown in Fig. 18. The filtering frequencies (dominant) were decided based on the frequency spectrum.

A LabVIEW™ virtual instrument was developed to filter using Butterworth lowpass 4^{th} order filter- with sampling frequency 200 Hz, low cut off frequency 16 Hz. Fig. 17 shows acceleration signal before and after filtering. There is an observable phase lag in the filtered with respect to the unfiltered signal.

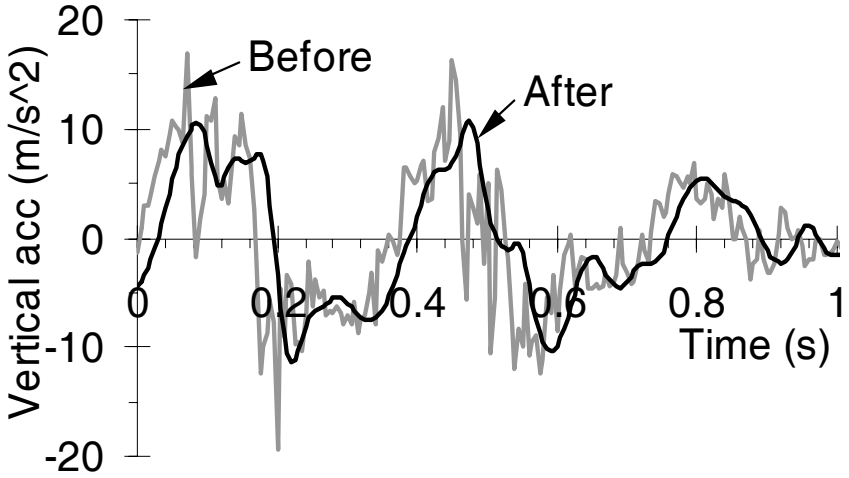

Fig. 17 Acceleration signal before and after filtering

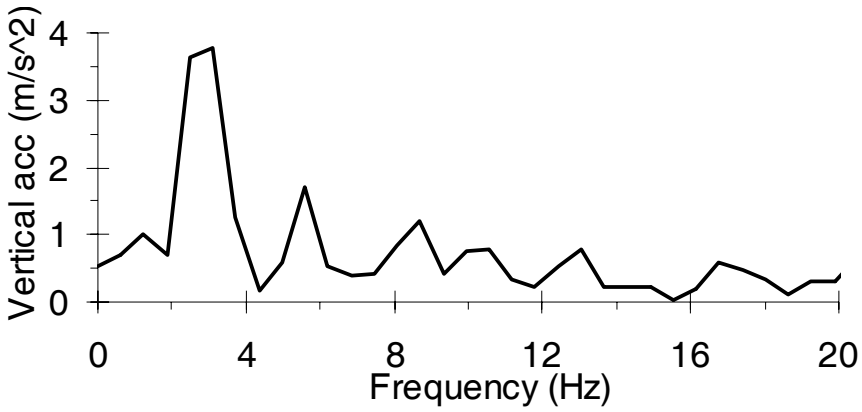

Fig. 18 FFT of the vertical acceleration signal

6 COMPARISON

Fig. 19 shows comparison of the experimental and simulation results in time domain. It can be seen that the results compared well with the theoretical predications except in the section after F where all wheels complete travel over the bump. After F, maximum upward acceleration is 5.5 m/s^2 by experimentation and 13.5 m/s^2 by simulation. It is thought that the variation in TWV structure stiffness is causing this. Unlike the model, the body of TWV is not rigid and is capable of some elastic deformations. Additionally elements like, rubber bushes, bearings at the kinematic joints and joint friction present in the load path that have not been modeled could be significant in the hard impact.

In section E-F, the upward acceleration observed to be decreasing continuously until all wheels complete the pass over bump. The rear wheels descend on the bump and the suspension is fully extended so TWV body goes down under gravitational force only. But in case of experimental plot in the same section the vertical acceleration is found to be fluctuating. The suspension is interposed between the wheels and the vehicle body. The wheel forces in addition to gravitational forces may be pulling the TWV body downward.

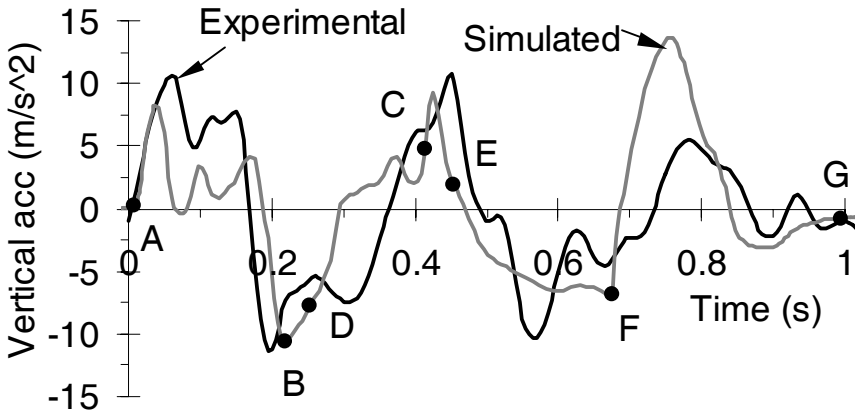

Fig. 19 Comparison of simulation and experimental results

The bump on which the tests were done, like most bumps in India, are made manually. The cross section of the bump is not invariant. The bump profile at the zone over which the front wheel

went was measured and used in simulation. It is to be expected that there will be a variation in the bump profile seen by the other two wheels.

7 CONCLUSION

A spatial six-DOF model of TWV with suspension and compliant tires is developed. The theoretical approach adopted for model building has been detailed. The mathematical methodology presented integrates the Euler's Equations explicitly and is hence valid for large displacement analysis. Events like wheel lift-off and limits of the suspension travel are explicitly accounted for in the simulation.

The instrumented TWV was run over road bumps (causing large vertical displacement) and measured vertical acceleration compared with the results of TWV mathematical model for validation. A good match is obtained, validating the simulation.

Using the steady state circular test procedure the lateral motion is validated. A constant steering angle input causes the TWV to follow the circular path. The radius of the which matches with the analytical results derived from geometry of TWV and shows the understeer charactristics. It is proposed to use the model to study the stability of the three-wheeled vehicle during NHTSA J-Turn, Fishhook maneuver and double lane change maneuver, and over other road irregularities.

REFERENCES

1. DeLisle, A., Laberge-Nadeau, C. and Brown, B. Characteristics of Three- and Four-Wheeled All-Terrain Vehicle Accidents in Quebec. *Accid. Anal. & Prev.*, **20**(5), 1988, pp. 357-366.
2. Crolla, D.A. Vehicle Dynamics—Theory into Practice. *Proc. Instn. Mech. Engrs., Automobile Engg.*, **210**(D2), 1996, pp. 83-94.
3. Tan, T.E. and Huston, J.C. Three-Wheeled ATV–A No-Suspension Rigid Rider System, Part I: Modeling and Parameter Values. *SAE 1984 Trans.*, Paper No. 841058, **93**(4), 1984, pp. 4.806-4.817.
4. Tan, T.E. and Huston, J.C. Three-Wheeled ATV–A No-Suspension Rigid Rider System, Part II: Applications-Handling and Ride. *SAE 1984 Trans.*, Paper No. 841059, **93**(4), 1984, pp. 4.818-4.824.
5. Ramji, K. and Goel, V.K. Vertical Dynamic Analysis of Three-wheeled Motor-vehilcles. *Journal of Institution of Engineers (India)*, **83**, 2002, pp. 40-51.
6. Ramji, K., Deep, K. and Goel, V.K. Optimum design of a three-wheeled vehicle suspension system subjected to random road excitation. *National Conference on Transportation Systems (NCTS)*, IIT Delhi, April 24-26, 2002, Transportation systems: Status and directions, 2002, pp. 682-686.
7. Ramji, K. and Goel, V.K. Ride characteristics of Three-wheeled motor vehicles. *Proceedings 17th National convention of mechanical engineers*, Indore, 26-27 Nov 2001, Mech. Engineering update and challenges ahead, 2001, pp. 243-252.
8. Shames, I.H. *Engineering mechanics- Static's and dynamics*, fourth edition, Prentice-Hall of India Pvt. Ltd., New Delhi, 1996, pp. 911-960.
9. Gillespie, T.D. *Fundamentals of vehicle dynamics*. SAE, Inc., Warrendale, 1992, pp.110-120 and pp. 198-199.
10. MADYMO theory manual. Version 5.4, TNO Automotive, 1999, pp. 243-258.
11. Singh, D.V., Goel, V.K. and Bhattcharya M. Rolling characteristics of small size pneumatic tyres, *The Inst. of Mech. Engrs.*, Auto. Div., **188**, 1974, pp.701-713.
12. Ellis, J.R. *Vehicle dynamics*. 1969, Business books Ltd. London, pp. 61.

13. Data, S., Frigerio, F. Objective evaluation of handling quality. *Proc. Instn. Mech. Engrs., Automobile Engg.*, **216**(D4), 2002, pp.297-305.

14. Anthropometric source book volume I: Anthropometry for designers. NASA reference publication 1024, Ed. By Staff of anthropology research project, Ohio, July 1978, pp. IV1-IV76.

APPENDIX A

FE model of TWV was developed in PAM-CRASH^{TM} using the drawings available from the manufacturer. The weight distribution was done based on the field measurements of individual parts of TWV. The CG lies in a frame (referred as $X_0Y_0Z_0$ *here after*) whose origin is at the center of track width and on the ground below the rear axle. The frame $X_0Y_0Z_0$ is aligned with the body-attached frame. CG location of empty TWV is given by (A1).

$$[x_3, y_3, z_3] = [0.556, 0, -0.492]\ m \quad \text{(A1)}$$

Mass moments of inertia, about an axis passing through CG, of empty TWV are known from the FE model developed and is given by (A2)

$$[I_{3xx}, I_{3yy}, I_{3zz}] = [54, 145.91, 150.52]\ kg.m^2 \quad \text{(A2)}$$

Each occupant of TWV is having weight of 70 kg and height of 66.93 in. Regression equations for predicting moments of inertia about an anatomical axis for driver in sitting configuration ($I_{1xx}, I_{1yy}, I_{1zz}$) and passenger in mercury configuration ($I_{2xx}, I_{2yy}, I_{2zz}$) are given are as follows **[14]**:

$$I_{1xx} = (1.43S + 0.322W - 91.6)^* 0.1131 = 6.085\ kg.m^2 \quad \text{(A3)}$$

$$I_{1yy} = (2.26S + 0.268W - 135.0)^* 0.1131 = 6.517\ kg.m^2 \quad \text{(A4)}$$

$$I_{1zz} = (0.76S + 0.201W - 52.8)^* 0.1131 = 3.289\ kg.m^2 \quad \text{(A5)}$$

$$I_{2xx} = (1.57S + 0.308W - 94.3)^* 0.1131 = 6.595\ kg.m^2 \quad \text{(A6)}$$

$$I_{2yy} = (2.85S + 0.318W - 175.0)^* 0.1131 = 7.331\ kg.m^2 \quad \text{(A7)}$$

$$I_{3zz} = (0.668S + 0.197W - 45.0)^* 0.1131 = 3.405\ kg.m^2 \quad \text{(A8)}$$

Where S is the stature in inches and W is the weight in pounds. The CG location for driver and passenger are as follows:

$$[x_{1b}, y_{1b}, z_{1b}] = [20.07, 0, 23.27]\ cm \quad \text{(A9)}$$

$$[x_{2b}, y_{2b}, z_{2b}] = [20.07, 0, 20.5]\ cm \quad \text{(A10)}$$

x_{1b}, x_{2b} are measured from the back plane, y_{1b}, y_{2b} are measured from the plane of symmetry (Sagittal), and z_{1b}, z_{2b} are measured from the seat pan.

The location of CG of driver (x_1, y_1, z_1) and CG of passenger (x_2, y_2, z_2) in TWV's $X_0Y_0Z_0$ frame are calculated using Bajaj Three Wheeler drawings and CG of occupants in their own frames. Those are as follows:

$$[x_1, y_1, z_1] = [1.105, 0, -0.875]\ m \quad \text{(A11)}$$

$$[x_2, y_2, z_2] = [0.335, 0, -0.915]\ m \quad \text{(A12)}$$

Center of gravity of TWV with n (=3) mass system, in $X_0Y_0Z_0$ frame is given by $[x_0, y_0, z_0]$ as follows:

$$x_0 = \frac{\sum_{i=1}^{n} m_i x_i}{m_0},\ y_0 = \frac{\sum_{i=1}^{n} m_i y_i}{m_0},\ z_0 = \frac{\sum_{i=1}^{n} m_i z_i}{m_0} \quad \text{(A13)}$$

Where m_i = mass of i^{th} body and $[x_i, y_i, z_i]$ = centre gravity of i^{th} body, i = 1, 2, 3.

After substitution of the values for individual masses and thieir locations in the $X_0Y_0Z_0$ frame, the CG of the total system (TWV and its occupants) is given by (A14).

$$[x_0, y_0, z_0] = [0.61, 0, -0.62]\ m \quad \text{(A14)}$$

Mass moment of Inertia of TWV with *n* (=3) mass system, [I_{xx}, I_{yy}, I_{zz}] is given by

$$I_{xx} = I_{1xx} + m_1(y_{1n}^2 + z_{1n}^2) + I_{2xx} + m_2(y_{2n}^2 + z_{2n}^2) + I_{3xx} + m_3(y_{3n}^2 + z_{3n}^2) \quad \text{(A15)}$$

$$I_{yy} = I_{1yy} + m_1(x_{1n}^2 + z_{1n}^2) + I_{2yy} + m_2(x_{2n}^2 + z_{2n}^2) + I_{3yy} + m_3(x_{3n}^2 + z_{3n}^2) \quad \text{(A16)}$$

$$I_{zz} = I_{1zz} + m_1(x_{1n}^2 + y_{1n}^2) + I_{2zz} + m_2(x_{2n}^2 + y_{2n}^2) + I_{3zz} + m_3(x_{3n}^2 + y_{3n}^2) \quad \text{(A17)}$$

Where

$[x_{1n}, y_{1n}, z_{1n}]$ location of CG of driver in Gxyz frame,

$[x_{2n}, y_{2n}, z_{2n}]$ location of CG of rear passenger in Gxyz frame,

$[x_{3n}, y_{3n}, z_{3n}]$ location of CG of empty TWV in Gxyz frame.

Therefore mass moment of inertia of TWV system represented in Gxyz frame is given by (A18).

$$[I_{xx}, I_{yy}, I_{zz}] = [80.64, 195.66, 178.54]\ kg.m^2 \quad \text{(A18)}$$

Table 1 Parameter values for Bajaj-rear engine model simulation

Parameter	Value	Notation	Unit
Longitudinal distance of CG of TWV system from front axle	1.39	*a*	m
Longitudinal distance of CG of TWV system from rear axle	0.61	*b*	m
Lateral distance of left/right wheel from CG of TWV	0.575	*c*	m
Total mass of Vehicle including driver and a passenger	403.87	*m*	kg
Compression allowed for front suspension spring	0.012	c_{fa}	m
Compression allowed for rear left/right suspension spring	0.085	c_{rra} *or* c_{rla}	m
Height of vehicle CG from road surface	0.62	*h*	m
Tire stiffness-front	238260	k_{fw}	N/m
Tire stiffness-rear left/right	250490	k_{rlw} *or* k_{rrw}	N/m
Wheel base	2.0	*l*	m
Wheel radius	0.21	r_w	m
Cornering stiffness for front wheel	3885	w_r	N/rad
Cornering stiffness for rear left or right wheel	4050	w_{rl} or w_{rr}	N/rad